JACS
JOURNAL OF THE AMERICAN CHEMICAL SOCIETY
Article
pubs.acs.org/JACS

Boundaries of Anion/Naphthalenediimide Interactions: From Anion−π Interactions to Anion-Induced Charge-Transfer and Electron-Transfer Phenomena

Samit Guha, Flynt S. Goodson, Lucas J. Corson, and Sourav Saha*

Department of Chemistry and Biochemistry and Integrative NanoScience Institute, Florida State University, 95 Chieftan Way, Tallahassee, Florida 32306, United States

Supporting Information

ABSTRACT: The recent emergence of anion−π interactions has added a new dimension to supramolecular chemistry of anions. Yet, after a decade since its inception, actual mechanisms of anion−π interactions remain highly debated. To elicit a complete and accurate understanding of how different anions interact with π-electron-deficient 1,4,5,8-naphthalenediimides (NDIs) under different conditions, we have extensively studied these interactions using powerful experimental techniques. Herein, we demonstrate that, depending on the electron-donating abilities (Lewis basicity) of anions and electron-accepting abilities (π-acidity) of NDIs, modes of anion−NDI interactions vary from extremely weak non-chromogenic anion−π interactions to chromogenic anion-induced charge-transfer (CT) and electron-transfer (ET) phenomena. In aprotic solvents, electron-donating abilities of anions generally follow their Lewis basicity order, whereas π-acidity of NDIs can be fine-tuned by installing different electron-rich and electron-deficient substituents. While strongly Lewis basic anions (OH^- and F^-) undergo thermal ET with most NDIs, generating $NDI^{\bullet-}$ radical anions and NDI^{2-} dianions in aprotic solvents, weaker Lewis bases (AcO^-, $H_2PO_4^-$, Cl^-, etc.) often require the photoexcitation of moderately π-acidic NDIs to generate the corresponding $NDI^{\bullet-}$ radical anions via photoinduced ET (PET). Poorly Lewis basic I^- does not participate in thermal ET or PET with most NDIs (except with strongly π-acidic core-substituted dicyano-NDI) but forms anion/NDI CT or anion−π complexes. We have looked for experimental evidence that could indicate alternative mechanisms, such as a Meisenheimer complex or CH···anion hydrogen-bond formation, but none was found to support these possibilities.

1. INTRODUCTION

Conceived in theory[1] and confirmed experimentally,[2] anion−π interactions[1−3] have emerged as a new paradigm of anion-recognition chemistry[4] that, for a long time, relied primarily on hydrogen-bonding interactions[5] and Lewis acid (transition metal ions, boron, etc.) coordination[6] of anions. Mirroring cation−π interaction[7] (e.g., $Na^+{\cdot}C_6H_6$ complex) between a cation and an electron-rich π-system with a negative quadrupole moment, non-covalent interactions between anions and π-electron-deficient systems (π-acids) with positive quadrupole moments are broadly defined as anion−π interactions.[1−3] Several anion/π-acceptor complexes have come to light since the turn of the millennium, yet most anion−π (anion−quadrupole) interactions are so weak that they do not usually perturb electronic properties of the π-acceptors, nor do they generate any optical response.[2] Only a handful π-acceptors[8] display optical changes upon interacting with certain anions, and the resulting UV/vis absorption spectra show Mulliken dependence,[8,9] i.e., a linear relationship between the donor/acceptor (D/A) electronic transition energies (ν_{CT}) and their redox potentials. These anion/π-acceptor interactions[8] have been aptly attributed to charge-transfer (CT) interactions that essentially resemble π-donor/acceptor CT interactions.[10] Expanding the scope and boundary of anion−π interactions, we were the first to demonstrate[11] unique formal electron transfer (ET) from Lewis basic anions to π-acidic 1,4,5,8-naphthalenediimides (NDIs) under thermal and light-gated conditions that generated $NDI^{\bullet-}$ radical anions and NDI^{2-} dianions.

In the realm of donor/acceptor chemistry, [D·A] CT states and $[D^{\bullet+}{\cdot}A^{\bullet-}]$ ET states belong to the same energy continuum.[12] The manifestation of CT or ET depends on the relative energies of HOMO and LUMO levels of electron donors and acceptors, respectively, and their spectroscopic signals are quite distinctive. For instance, if the HOMO of an electron donor is located well above the LUMO of an electron acceptor (Figure 1a), the thermal ET pathway should be turned ON ($\Delta G^\circ_{ET} < 0$), generating paramagnetic $D^{\bullet+}$ and $A^{\bullet-}$ radical ions.[11b,12] In contrast, if the HOMO of an electron donor is located below the LUMO of an electron acceptor, thermal ET should be turned OFF ($\Delta G^\circ_{ET} > 0$, forbidden). However, if the donor HOMO is located above the photogenerated SOMO−1 of the electron acceptor, photoinduced electron-transfer (PET) pathway could be turned ON (Figure 1b), generating the same $A^{\bullet-}$ radical anion. Regardless of the electron source (electrochemical vs chemical reduction, thermal ET vs PET), a given $A^{\bullet-}$ radical anion always displays the same characteristic signals (UV/vis and EPR). The rate and extent of $A^{\bullet-}$ formation depend on the ET driving force (ΔG°_{ET} and ΔG°_{PET}). When

Received: April 2, 2012
Published: June 11, 2012

   dx.doi.org/10.1021/ja303173n | J. Am. Chem. Soc. 2012, 134, 13679−13691

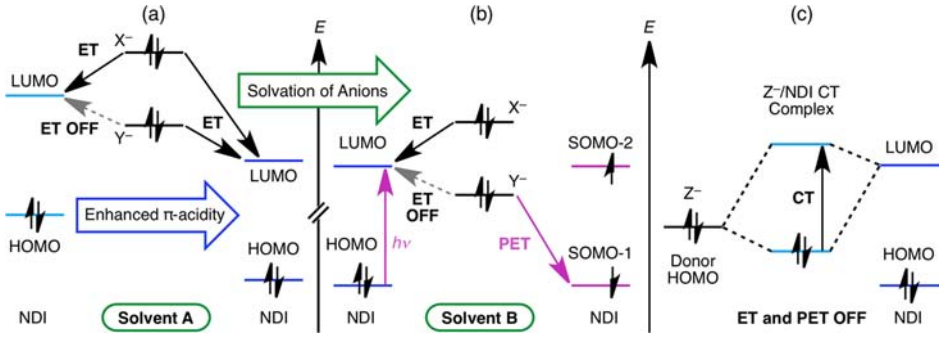

Figure 1. Energy diagrams show how the relative positions of the HOMO and LUMO levels of NDIs with respect to the HOMO of anions channel anion/NDI interactions through anion-induced (a) thermal ET ($\Delta G^\circ_{ET} < 0$), (b) PET ($\Delta G^\circ_{ET} \geq 0$, but $\Delta G^\circ_{PET} < 0$), and (c) CT interactions. (a) Thermal ET takes place when the HOMO of anion is located above the LUMO of NDI. (b) PET takes place when the HOMO of the anion lies below the LUMO of NDI but still above its HOMO. (c) CT interaction takes place when the anion is weakly Lewis basic and cannot trigger formal ET to NDIs. Lewis basicity trend: $X^- > Y^- \gg Z^-$.

both thermal and photoinduced ET are turned OFF because of a significantly low-lying donor HOMO level, neutral D/A CT complexes could be formed via orbital mixing (Figure 1c).[11b] CT complexes show broad UV/vis absorption bands, the locations of which (λ_{CT}) depend on the donor and acceptor strengths (Mulliken dependence).[8,10,12]

Given the similarities between π-donor/acceptor and anion/π-acceptor CT interactions and well-known examples of ascorbate-mediated reductions of the Lewis acidic transition metal ions, e.g., Fe(III) to Fe(II) in cytochrome-b redox protein[13] and Cu(II) to Cu(I) in "click chemistry",[14] the paucity of anion-induced formal ET to neutral π-acceptors seems quite surprising. Herein, we demonstrate that an anion can interact with a neutral π-acceptor through either non-chromogenic anion$-\pi$ interactions or chromogenic CT and ET interactions, if a delicate interplay between (1) the anion's Lewis basicity, i.e., electron-donating ability, (2) the π-acceptor's electron-accepting ability, and (3) the effects of solvents and counterions on the Lewis basicity of the anions satisfies the requirement of each mechanism. In addition to these anion/π-acceptor interactions, two other modes of contacts, namely, (i) CH···anion H-bonding[15] and (ii) covalent Meisenheimer or σ-complex[15a,16] formation, have also been debated within the realm of anion/π-acceptor interactions. In CH···anion H-bonding, the anion interacts with an acidic proton along the σ-frame rather than interacting with the positive quadrupole of the π-acceptor, a phenomenon that usually causes a downfield chemical shift of the H-bonded proton.[17] Nucleophilic attack of an anion on a π-acceptor could form a covalent σ-bond, and the resulting $[X{-}A]^-$ species is called a Meisenheimer complex.[18] Although Meisenheimer complexes often display vibrant colors, unlike EPR-active paramagnetic $A^{\bullet-}$ radical anions, these covalent $[X{-}A]^-$ intermediates are usually diamagnetic species.

While we demonstrated[11] formal ET from Lewis basic anions (e.g., F^-, AcO^-, $H_2PO_4^-$, and Cl^-) to tunable π-acidic NDI receptors under thermal and photoinduced conditions, Dunbar et al.[8c] demonstrated that π-acidic HAT$(CN)_6$ receptor forms CT complexes with halides, and Matile et al.[8d] reported formation of various anion/NDI complexes. In the latter two cases, π-acceptors displayed stronger affinity and selectivity toward more Lewis basic anions (e.g., $Cl^- > Br^- > I^-$). In addition to anion/NDI CT complexes, Matile et al.[8d] also observed a highly featured, new UV/vis spectrum of unsubstituted NDIs in the presence of strongly Lewis basic F^- and a similar spectrum of a strongly π-acidic core-substituted dicyano-NDI (DCNDI) in the presence of less basic I^-. While the sharp UV/vis spectrum resulting from I^-/DCNDI interaction was loosely attributed to CT or ET from I^- (although these two processes are fundamentally different,[12] *vide supra*), a $[F{-}NDI]^-$ Meisenheimer complex formation was invoked[8d] to rationalize similar spectroscopic changes induced by F^-. Electrospray ionization mass spectrometry (ESIMS) revealed a wide range of anion/π-acceptor $[X^-/A]$ adducts,[8d,11] which could be interpreted as one of the following possibilities: (1) $[X^-/A]$ complex formation via CT, ET, or anion$-\pi$ interaction, (2) $[X^{\bullet}/A^{\bullet-}]$ radical pair formation after an anion-induced ET, (3) CH···X^- H-bonded complex formation, or (4) covalent $[X{-}A]^-$ Meisenheimer complex formation. Although covalent Meisenheimer complex formation between electron-deficient dinitrotoluene and Lewis bases has been long believed to be the cause of ensuing colorimetric changes, Bühlmann et. al.[18b] recently demonstrated that, instead of forming Meisenheimer complex, OH^- and amines actually deprotonate an acidic proton from the Me group of DNT, generating an electron-delocalized, colorful anionic species. Furthermore, *ab initio* calculations[19] suggest that modes of anion/π-acceptor interactions vary drastically in the presence of different solvent molecules. For instance, a covalent F^-—triazine Meisenheimer complex or a CH···Cl^- H-bonded triazine·Cl^- complex constitutes the lowest-energy structure in the gas phase (no or little solvent), whereas anion$-\pi$ interaction becomes the most stable and preferable mode in the presence of solvent molecules (MeCN or H_2O).[19] Thus, insufficient studies and incomplete explanations caused further confusion in this highly debated field of anion$-\pi$ interactions.

In this article, we present a comprehensive analysis of different modes of anion/π-acceptor interactions through structure—property relationship studies using powerful experimental techniques, such as UV/vis, NMR, and EPR spectroscopies, electrochemistry, spectroelectrochemistry, isothermal titration calorimetry, and X-ray photoelectron spectroscopy (XPS). Density functional theory (DFT) and natural bond orbital calculations have also been used to identify the electron-deficient areas of NDIs and how they interact with different anions. These studies unequivocally show that, depending on the π-acidity of NDIs, the Lewis basicity of anions, solvents, and experimental conditions, modes of anion/NDI interactions vary from anion-induced thermal and light-gated ET phenomena to

dx.doi.org/10.1021/ja303173n | J. Am. Chem. Soc. 2012, 134, 13679−13691

Chart 1. Molecular Structures of NDI Derivatives

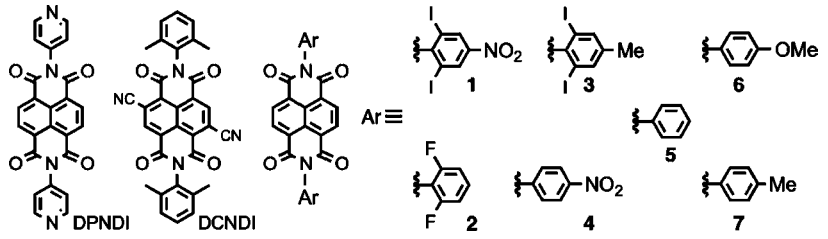

weak CT and anion−π interactions and rule out σ-complex formation and deprotonation of NDIs.

2. RESULTS AND DISCUSSION

To understand how electronic and structural parameters of anions and π-acceptors control the mechanisms of their interactions, we chose π-electron-deficient, neutral NDI compounds[20] as a common platform (Chart 1). The π-acidity of NDI receptors can be easily manipulated by installing different electron-rich and -deficient substituents on two imide N-centers[11b] as well as at the core naphthalene ring (cNDIs).[21] We have previously demonstrated[11] that N-substituents impart modest impacts on NDI's π-acidity, while others[8d,21] have demonstrated that electron-withdrawing core substituents render the corresponding cNDIs strongly π-acidic.

2.1. Synthesis and Characterization. The *N,N′*-disubstituted NDI derivatives (e.g., *N,N′*-dipyridyl NDI (DPNDI), NDIs **1**−**7**) have been synthesized by standard bis-imidization[11] of commercially available naphthalene-1,4,5,8-tetracarboxydianhydride (NDA) with corresponding amines (Supporting Information, Scheme S1). To prepare dicyano-substituted NDI (DCNDI), NDA was first brominated with dibromoisocyanuric acid according to a literature procedure (Scheme S2).[21] The corresponding dibromo-NDI was then treated with CuCN to afford DCNDI (Scheme S2).[8d,21c] All these compounds have been purified by column chromatography and characterized by NMR spectroscopies and high-resolution ESIMS. ^{1}H NMR signals of the central naphthalene protons of symmetric *N,N′*-disubstituted NDI derivatives appear as a singlet at δ ~8.8 ppm, whereas the characteristic singlet peak of strongly π-acidic DCNDI's core protons appears farther downfield at 9.07 ppm.

2.2. Electrochemistry. To quantify π-acidities of NDIs in different solvents, cyclic voltammograms were recorded in different polar (MeCN, DMF, and DMSO) and nonpolar (*o*-dichlorobenzene (ODCB)) solvents. In both polar and nonpolar solvents, the trend of NDI's π-acidity remains the same (Figure S1); however, polar solvents render the reduction of NDIs slightly easier than nonpolar solvents, a phenomenon that can be attributed to better stabilization of negatively charged NDI$^{\bullet-}$ and NDI^{2-} species in polar media. HOMO and LUMO energies of NDIs have been calculated from their redox potentials (E^1_{Redox}) and electronic absorption spectra using the following equations:[21c]

$$E_{\mathrm{HOMO}} = [-4.8\ \mathrm{eV} - (E^1_{\mathrm{Ox}} - 0.42)(\mathrm{V})]\ \mathrm{eV} \quad (1)$$

$$E_{\mathrm{LUMO}} = [-4.8\ \mathrm{eV} - (E^1_{\mathrm{Red}} - 0.42)(\mathrm{V})]\ \mathrm{eV} \quad (2)$$

$$\Delta E_{\mathrm{HOMO-LUMO}} = 1240/\lambda_{\mathrm{onset}} \quad (3)$$

when the redox potentials are measured against a Ag/AgCl reference electrode. CV data show that the electron-withdrawing substituents enhance the π-acidity of NDIs, as they display less negative first reduction potentials (E^1_{Red}) and lower LUMO levels, whereas electron-rich substituents diminish π-acidity, render the corresponding NDIs more difficult to reduce, and elevate their LUMO levels (Table 1). While the N-substituents impart a modest impact on NDI's π-acidity, which is evident from more subtle changes in reduction potentials, electron-withdrawing cyano- groups at the NDI core dramatically enhance its π-acidity. The low-lying LUMO levels of strongly π-acidic NDIs open up the possibility of ET from several electron donors that possess higher HOMO levels, rendering ET events less selective (Figure 1a). On the other hand, moderately π-acidic NDIs possessing higher LUMO levels are expected to undergo ET more selectively only from the stronger Lewis basic anions (e.g., F$^-$, OH$^-$, CN$^-$, etc.).

Table 1. NDIs' Redox Potentials (vs Ag/AgCl in MeCN), HOMO, and LUMO Energies

NDIs	$E^1_{\mathrm{Red}}/E^2_{\mathrm{Red}}$ (mV)	LUMO/HOMO (eV)
DCNDI	+10/−500	−4.39/−7.49
NDI **1**	−310/−790	−4.07/−7.17
NDI **2**	−380/−830	−4.00/−7.10
NDI **3**	−395/−885	−3.98/−7.08
DPNDI	−440/−890	−3.94/−7.04
NDI **4**	−510/−900	−3.87/−6.97
NDI **5**	−535/−965	−3.85/−6.95
NDI **6**	−550/−975	−3.83/−6.93
NDI 7	−560/−980	−3.82/−6.92

2.3. Spectroelectrochemistry. To characterize UV/vis absorption properties of NDI$^{\bullet-}$ and NDI^{2-} species, we conducted spectroelectrochemical analysis of NDIs using nonbasic $Bu_4N^+PF_6^-$ ($TBAPF_6$) as a supporting electrolyte. Constant potentials (V_{ap}) commensurate with the first and second reduction potentials were applied until NDI$^{\bullet-}$ and NDI^{2-} spectra became saturated in stepwise fashion. Electrochemical oxidation of NDI$^{\bullet-}$ and NDI^{2-} regenerated neutral NDIs as the original spectra reappeared, demonstrating complete reversibility of redox processes.

Regardless of the substituents, all neutral NDIs (DPNDI, DCNDI, and NDIs **1**−**7**) are colorless compounds that absorb in the UV region (340−400 nm), indicating that these substituents do not significantly modify HOMO−LUMO band gaps. However, NDI$^{\bullet-}$ radical anion and NDI^{2-} dianion are intensely colorful species that display highly featured UV/vis absorption spectra spanning across the visible−NIR region (Figures 2a and S2).[11,22] For instance, electrochemical reduction of colorless DPNDI (λ_{Abs} = 343, 361, and 381 nm) to an orange colored DPNDI$^{\bullet-}$ at V_{ap} = −450 mV (vs Ag/AgCl) produces highly featured absorption spectrum that displays prominent new peaks at 475 (λ_{max}), 605, 711, and 791 nm and diminished intensities of the neutral DPNDI peaks in

dx.doi.org/10.1021/ja303173n | J. Am. Chem. Soc. 2012, 134, 13679−13691

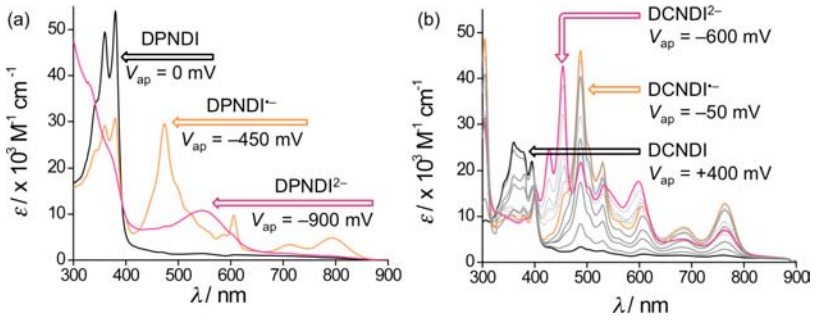

Figure 2. Spectroelectrochemical analysis of (a) DPNDI (in 0.1 M $TBAPF_6$/DMF) and (b) DCNDI (in 0.1 M $TBAPF_6$/MeCN). UV/vis spectra of (a) neutral DPNDI (V_{ap} = 0 mV, black trace), $DPNDI^{\bullet-}$ (V_{ap} = −450 mV, orange trace), and $DPNDI^{2-}$ (V_{ap} = −900 mV, pink trace), and (b) neutral DCNDI (V_{ap} = +400 mV, black trace), $DCNDI^{\bullet-}$ (V_{ap} = −50 mV, orange trace), and $DCNDI^{2-}$ (V_{ap} = −600 mV, pink trace).

the UV-region, establishing a clear isosbestic point at 394 nm (Figure 2a). Further reduction of $DPNDI^{\bullet-}$ to a pink colored $DPNDI^{2-}$ dianion at V_{ap} = −900 mV (vs Ag/AgCl) made $DPNDI^{\bullet-}$ signals disappear and a prominent new peak appear at 542 nm. All $NDI^{\bullet-}$ radical anions constitute a doublet state (D_0) and their longer wavelength absorption peaks correspond to $D_0 \rightarrow D_1$ electronic transitions.[22] Absorption features of all $NDI^{\bullet-}$ and NDI^{2-} species obtained from different *N,N′*-disubstituted NDIs are essentially the same (Figure S2), with slight differences in peak positions (ca. ± 5 nm), indicating that electrons are delocalized only within the NDI core and not through the N-substituents.

Using spectroelectrochemical analysis, for the first time, we were able to identify the spectroscopic signatures of $DCNDI^{\bullet-}$ radical anion and $DCNDI^{2-}$ dianion upon stepwise electrochemical reduction of DCNDI (Figure 2b). Since electron-withdrawing cyano substituents are in conjugation with the central π-system, the $DCNDI^{\bullet-}$ and $DCNDI^{2-}$ spectra are significantly different from those displayed by reduced *N,N′*-disubstituted NDIs. While neutral DCNDI absorbs light at 342, 358 (λ_{max}), 379, and 394 nm, the electrochemically generated $DCNDI^{\bullet-}$ radical anion (V_{ap} = −50 mV) displays significantly diminished intensity of these signals and prominent new peaks at 401, 454, 487 (λ_{max}), 530, 605, 686, and 764 nm, establishing a clear isosbestic point at 400 nm. The second reduction, leading to $DCNDI^{2-}$ dianion formation (V_{ap} = −600 mV), diminishes the intensities of 487, 530, 686, and 764 nm peaks of $DCNDI^{\bullet-}$ radical anion and generates new peaks at 427, 454 (λ_{max}), and 532 nm, establishing clear isosbestic points at 400, 465, 540, and 615 nm (Figure 2b). Electrochemical oxidation of $DCNDI^{2-}$ dianion to neutral DCNDI (V_{ap} = +100 mV) takes place via an intermediate $DCNDI^{\bullet-}$ formation, as $DCNDI^{\bullet-}$ signal emerges momentarily at the expense of $DCNDI^{2-}$ spectrum before disappearing to regenerate the original DCNDI spectrum. This new information is critical for an accurate understanding of anion-induced spectroscopic changes in NDIs and cNDIs, lack of which misled researchers[8d] to prematurely attribute F^--induced spectroscopic changes of NDIs to a covalent $[F-NDI]^-$ Meisenheimer complex formation. In the following sections, we will show that electrochemically generated $NDI^{\bullet-}$ radical anion and NDI^{2-} dianion spectra, including the isosbestic points, are identical to those generated by Lewis basic anions.

2.4. UV/Vis Studies of Anion/NDI Interactions. To understand how the interplay between the π-acidity of NDIs and Lewis basicity of anions regulates different modes of anion/NDI interactions, we surveyed the interactions of a library of NDI derivatives—DPNDI, DCNDI, and NDIs **1**−**7** (Chart 1)—with Bu_4N^+ (TBA) and Et_4N^+ (TEA) salts of various anions with decreasing Lewis basicity: $OH^- > F^- > CN^- > AcO^- > H_2PO_4^- > Cl^- > Br^- > I^- \gg PF_6^-$.[23] By adjusting the Lewis basicity of anions and π-acidity of NDIs, anion-induced ET to NDIs can be channeled through two distinct pathways (Figure 1a).[11b] (1) When anion and NDI are strong electron donors and acceptors, respectively, the HOMO of the anion is located above the LUMO of NDI, a situation that turns ON a thermal anion-to-NDI ET. (2) When the HOMO of a less Lewis basic anion falls below the LUMO of an NDI but still rests above its HOMO, the thermal ET is turned OFF, but light can activate a PET pathway from the anion's HOMO to the photogenerated ^{1}*NDI's SOMO−1. The final electronic configurations of $NDI^{\bullet-}$ and NDI^{2-} species generated by direct electrochemical reduction or anion-induced ET are the same. Therefore, irrespective of the electron source, the reduced NDI species display identical spectroscopic signals. When anions are poor electron donors but highly polarizable (e.g., I^- and Br^-), anion-induced ET and PET to NDIs are turned OFF, but CT and anion−π interactions could still take place.

Thermal Anion-Induced Electron Transfer to N,N′-Disubstituted NDIs. UV/vis titration of a moderately π-acidic DPNDI (E^1_{Red} = −450 mV vs Ag/AgCl) in DMSO with strongly basic anions, e.g., OH^- (pK_a of H_2O in DMSO = 32), F^- (pK_a of HF in DMSO = 15), and CN^- (pK_a of HCN in DMSO = 13) gradually bleached the original DPNDI absorption peaks at 343, 361, and 381 nm and concurrently produced prominent new peaks at 475 (λ_{max}), 605, 711, and 791 nm, establishing a clear isosbestic point at 394 nm (Figures 3 and S3) as the solution turned orange. The entire spectrum, including the isosbestic point (394 nm) of F^--generated orange solutions of DPNDI, is essentially identical to that of the electrochemically generated $DPNDI^{\bullet-}$ radical anion produced in the absence of these anions (Figures 2a and 3b, orange traces), suggesting that $DPNDI^{\bullet-}$ radical anion is formed via an ET from strongly Lewis basic anions.[11a] Had the anion reacted with DPNDI as a nucleophile, forming a covalent [anion−DPNDI]$^-$ Meisenheimer complex en route $DPNDI^{\bullet-}$ formation, the isosbestic point (394 nm) during anion titrations should have been different from that observed during electrochemical generation of $DPNDI^{\bullet-}$ radical anion, as these two pathways would have been completely different.

Addition of higher equivalents of F^- (also OH^- and CN^-, Figure S3) turned the orange-colored $DPNDI^{\bullet-}$ solution to pink that displayed gradual disappearance of the characteristic $DPNDI^{\bullet-}$ signals with a concomitant emergence of a new peak at 542 nm (Figure 3b, pink trace). UV/vis spectra of anion-

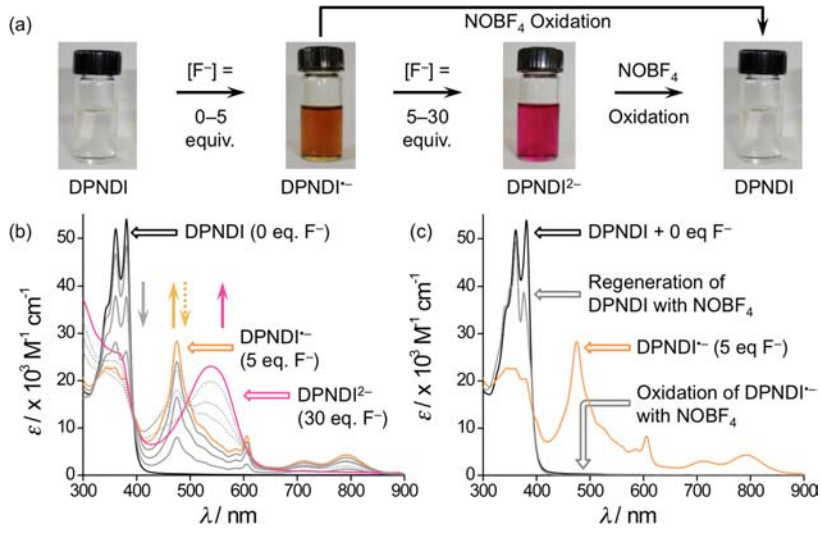

Figure 3. F^--induced (a) colorimetric and (b,c) UV/vis spectroscopic changes of DPNDI in DMSO from colorless (no F^-) to orange (≤5 equiv of F^-) to pink (5–30 equiv of F^-) and back to colorless upon $NOBF_4$ treatment of colored solutions. (b) UV/vis titration of DPNDI with F^- ($TBAF{\cdot}3H_2O$). Black trace, neutral DPNDI (no F^-); orange trace, $DPNDI^{\bullet-}$ (5 equiv of F^-); and pink trace, $DPNDI^{2-}$ (30 equiv of F^-). (c) Regeneration of neutral DPNDI spectrum upon oxidation of $DPNDI^{\bullet-}$ with $NOBF_4$.

generated pink solutions of DPNDI closely resemble an electrochemically generated $DPNDI^{2-}$ dianion spectrum (Figures 2a and 3b), suggesting the formation of $DPNDI^{2-}$ in the presence of excess amounts of strongly Lewis basic anions. ESIMS and ITC studies (*vide infra*) further demonstrate the formation of a 1:1 $F^-{\cdot}DPNDI$ complex (m/z = 439.1). Although ESIMS data could be interpreted as a $[F^-{\cdot}DPNDI]$ precursor complex formation prior to the first ET or a $[F^{\bullet}{\cdot}DPNDI^{\bullet-}]$ radical-pair complex formation as a result of ET, UV/vis and EPR (*vide infra*) studies do not display any electronic perturbation of $DPNDI^{\bullet-}$ with F^- or $F^{\bullet}$. Anion-induced formation of $DPNDI^{2-}$ dianion was also observed through ESIMS (m/z = 210.9). Due to electrostatic repulsions, it is extremely unlikely that the reduction of $DPNDI^{\bullet-}$ to $DPNDI^{2-}$ with a second equivalent of strongly Lewis basic anions would proceed through complexation of an anion with $DPNDI^{\bullet-}$, leaving outer-sphere ET as the only possible mechanism of the second reduction.

Akin to completely reversible electrochemical reductions of DPNDI (DPNDI ⇆ $DPNDI^{\bullet-}$ ⇆ $DPNDI^{2-}$), the anion-generated $DPNDI^{\bullet-}$ and $DPNDI^{2-}$ species can be fully oxidized back to neutral DPNDI using an oxidizing agent, $NOBF_4$, that regenerates the original DPNDI spectrum (Figure 3c). A neutral reducing agent, NH_2NH_2, also generates $DPNDI^{\bullet-}$ radical anion but cannot form $DPNDI^{2-}$ (Figure S3), possibly because of its weaker reducing ability than strongly Lewis basic anions. Thus, strong similarities between chemically generated, electrochemically generated, and anion-generated $DPNDI^{\bullet-}$ and $DPNDI^{2-}$ spectra corroborate that all these ET pathways are equivalent and that no covalent Meisenheimer intermediate is involved. Weaker Lewis basic anions, e.g., AcO^-, $H_2PO_4^-$, Cl^-, Br^-, I^-, and PF_6^-, do not reduce DPNDI at all, as the spectra of DPNDI in the presence of large excesses of these anions remain unchanged (Figure S4). The fact that, in aprotic solvents strongly Lewis basic anions (OH^-, F^-, and CN^-) generate $DPNDI^{\bullet-}$ and $DPNDI^{2-}$, but less basic anions (AcO^-, $H_2PO_4^-$, ClO_4^-, Cl^-, Br^-, I^-, and PF_6^-) do not, clearly shows that the former anions have much better electron-donating ability than the latter ones. In protic solvents (H_2O and MeOH), F^- no longer generates $DPNDI^{\bullet-}$ and $DPNDI^{2-}$, a phenomenon that can be attributed to high solvation of small F^- ion via H-bonding interactions ($-\Delta H_{Hydration}$ of F^- = 115 kcal/mol),[24] which dramatically diminishes its Lewis basicity and electron-donating ability.

Thermal Anion-Induced Electron Transfer to DCNDI. Because of strong π-acidity of DCNDI, electron-rich neutral solvents, such as DMSO, DMF, and DMAc, undergo thermal ET, generating $DCNDI^{\bullet-}$ spectra (Figure S5), rendering these solvents unsuitable for the investigation of anion/DCNDI interactions. To avoid solvent-mediated ET and PET, freshly prepared MeCN solutions of DCNDI were titrated with anions in the absence of light.

As in the case of spectroelectrochemical analysis, UV/vis titrations of DCNDI with strongly Lewis basic F^- and OH^- ions initially diminish the neutral DCNDI peaks at 342, 358 (λ_{max}), 379, and 394 nm and generate prominent new peaks at 401, 454, 487 (λ_{max}), 530, 605, 686, and 764 nm, establishing a clear isosbestic point at 400 nm (Figure 4a,b). Addition of more than 1 equiv of these anions diminishes the intensities of $DCNDI^{\bullet-}$ radical anion peaks at 487, 530, 686, and 764 nm and generates new peaks at 427, 454 (λ_{max}), and 532 nm, establishing new isosbestic points at 400, 465, 540, and 615 nm. The second step corresponds to $DCNDI^{2-}$ dianion formation. While strongly Lewis basic anions (F^- and OH^-) generate up to $DCNDI^{2-}$ dianion in two steps, weaker Lewis basic anions, e.g., AcO^-, Cl^-, Br^-, and I^-, that do not reduce moderately π-acidic DPNDI at all, can only produce $DCNDI^{\bullet-}$ radical anion but do not generate $DCNDI^{2-}$ dianion via thermal ET (Figures 4c and S5). $NOBF_4$ oxidizes anion-generated $DCNDI^{\bullet-}$ and $DCNDI^{2-}$ species back to neutral DCNDI, as the original spectrum reappears (Figure S5).

If F^- and OH^- ions indeed formed covalent Meisenheimer complexes with NDIs, cleavage of these σ-bonds under oxidative ($NOBF_4$) conditions to regenerate neutral NDI would be an unlikely event. The similarities between reversible spectroscopic changes under electrochemical conditions and with anions corroborate that anion-induced thermal ET events are indeed responsible for $DCNDI^{\bullet-}$ and $DCNDI^{2-}$ formation and no Meisenheimer complex is involved.

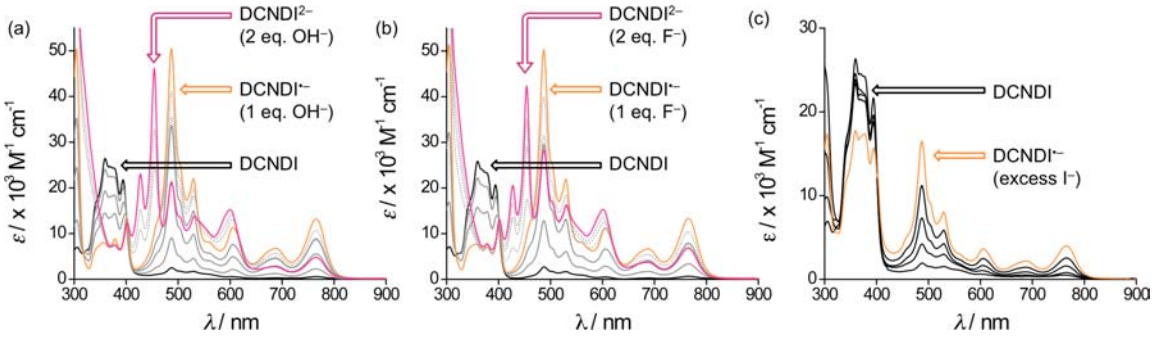

Figure 4. UV/vis spectroscopic changes of DCNDI in MeCN (black trace) upon two-step reduction to $DCNDI^{\bullet-}$ (orange trace) and $DCNDI^{2-}$ (pink trace) with (a) OH^- and (b) F^-, and (c) one-step reduction to $DCNDI^{\bullet-}$ with 100 equiv of I^-.

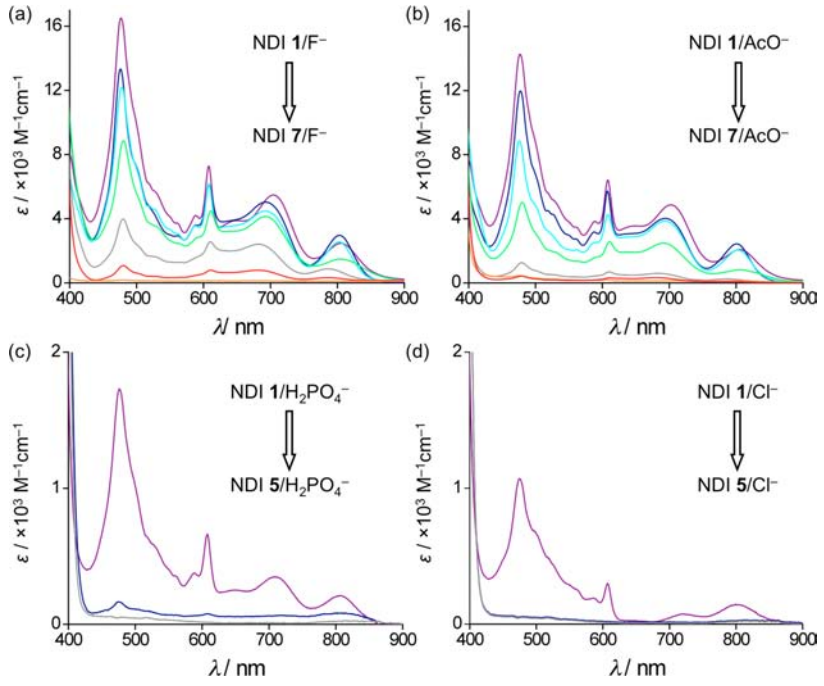

Figure 5. Anion-generated UV/vis spectra of $NDI^{\bullet-}$ radical anions of NDIs **1** (violet), **2** (indigo), **3** (cyan), **4** (green), **5** (gray), **6** (red), and **7** (orange) (each 30 μM in ODCB) in the presence of (a) F^- (10 equiv), (b) AcO^- (50 equiv), (c) $H_2PO_4^-$ (50 equiv), and (d) Cl^- (100 equiv). The spectra show that while (a) F^- and (b) AcO^- generate $NDI^{\bullet-}$ radical anions of **1**−**7**, (c) $H_2PO_4^-$ does so only for NDIs **1** and **2**, and (d) Cl^- does so only for NDI **1**. The extent of $NDI^{\bullet-}$ formation diminishes with decreasing π-acidity of NDIs and Lewis basicity of anions.

Regulating Anion-Induced Thermal ET. To examine whether anion-induced thermal ET to NDIs can be turned ON/OFF by adjusting the π-acidity (LUMO level) of NDIs with respect to Lewis basicity (HOMO level) of anions, we surveyed the interactions between NDIs **1**−**7** with gradually decreasing π-acidity and F^-, AcO^-, $H_2PO_4^-$, and Cl^- ions with gradually decreasing Lewis basicity.[11b] UV/vis titrations of NDIs **1**−**7** in ODCB with strongly Lewis basic F^- generate prominent $NDI^{\bullet-}$ spectra (Figure 5a), however, as the π-acidity of NDIs gradually diminishes, the extent of $NDI^{\bullet-}$ formation decreases. Similarly, as the Lewis basicity of anions decreases ($F^- > AcO^- > H_2PO_4^- > Cl^-$),[8c,11b,23] their electron-donating abilities and HOMO levels diminish,[8c] first weakening and eventually turning OFF thermal ET to NDIs (Figure 1a). As a result, less basic AcO^- generates weaker $NDI^{\bullet-}$ signals from NDIs **1**−**7** (Figure 5b) than those produced by F^-, while $H_2PO_4^-$ generates very weak $NDI^{\bullet-}$ signals only with NDI **1**−**4** (Figure 5c), and Cl^- triggers extremely weak thermal ET only to NDI **1** in ODCB (Figure 5d). Regardless of the N-substituents, anion-generated $NDI^{\bullet-}$ absorption spectra and isosbestic points are essentially identical to those of electrochemically generated $NDI^{\bullet-}$ radical anions in the absence of any electron-donating anions, confirming that anion-to-NDI ET events are indeed responsible for these spectroscopic changes and ruling out a Meisenheimer complex formation. In summary, the extent of anion-induced $NDI^{\bullet-}$ formation is greater when the energy gap (ΔG°_{ET}) between the anion's HOMO and the NDI's LUMO is larger. ΔG°_{ET} decreases as anions and NDIs become weaker electron donors and acceptors, respectively, diminishing the $NDI^{\bullet-}$ radical anion formation via thermal ET.

Photoinduced Electron Transfer from Anions to N,N′-Disubstituted NDIs. Next, we turned our attention to explore whether a PET from the HOMO of an anion to the SOMO−1 of the ^{1*}NDI excited state (Figure 1b) could generate $NDI^{\bullet-}$ radical anion when thermal anion-to-NDI ET is turned OFF.[11b] Solvents have an important effect on anion's Lewis basicity. Protic solvents (H_2O, MeOH) and aprotic solvents containing acidic protons (MeCN) can better solvate anions through H-bond formation, which diminishes anions' Lewis basicity and

dx.doi.org/10.1021/ja303173n | J. Am. Chem. Soc. 2012, 134, 13679−13691

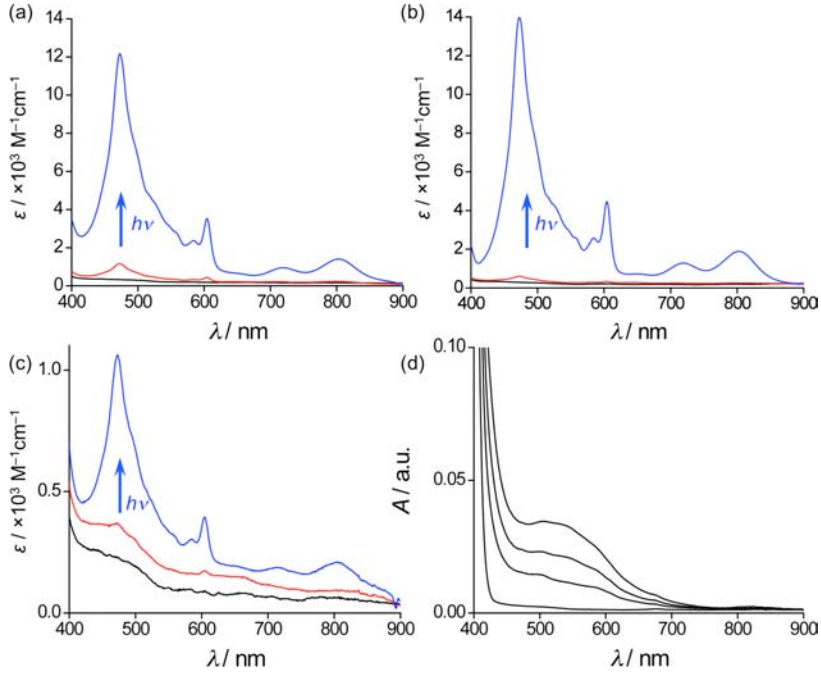

Figure 6. (a–c) UV/vis spectra of NDI **1** in MeCN in the absence of any anion (black traces) and in the presence of large excess (≥50 equiv) of (a) AcO^-, (b) $H_2PO_4^-$, and (c) Cl^-, showing negligible $\mathbf{1}^{\bullet-}$ formation in the dark (red traces). Irradiation of these solution mixtures (a–c) with a W-lamp significantly enhances the $\mathbf{1}^{\bullet-}$ signals (blue traces) upon anion-mediated photoreduction of ^{1}*NDI **1**. (d) At high concentrations (0.5 mM), NDI **1** displays CT absorption band with excess I^- (100 equiv) but does not form any $\mathbf{1}^{\bullet-}$.

electron-donating ability.[8c,11b] Therefore, while AcO^-, $H_2PO_4^-$, and Cl^- anions could trigger thermal ET to several NDIs in ODCB (Figure 5), many of these thermal ET pathways are turned OFF in MeCN (Figure 6), which opened up the possibility of PET. To test this hypothesis, we irradiated the NDI solutions in the presence of anions that showed negligible or no $NDI^{\bullet-}$ formation in the dark (no thermal ET) with a W-lamp and periodically recorded UV/vis spectra.

Irradiation of a MeCN solution of NDI **1** in the presence of AcO^-, $H_2PO_4^-$, and Cl^-, which originally showed extremely weak or no thermal ET interaction, immediately turns ON the anion-to-^{1}*NDI PET, significantly enhancing the intensity of NDI $\mathbf{1}^{\bullet-}$ absorption spectra that reached saturation within 10 min of irradiation (Figure 6a–c).[11b] Similarly, NDIs **2**–**4** undergo PET from AcO^- and $H_2PO_4^-$ in MeCN (Figure S6). Anion-induced PET to NDI is also observed in ODCB when a thermal ET is negligible or turned OFF. For instance, in ODCB, NDIs **6** and **7** undergo photoreduction with AcO^- and NDIs **1**–**5** with $H_2PO_4^-$, generating characteristic $NDI^{\bullet-}$ radical anion signals (Figure S7). When a facile thermal anion-to-NDI ET process generates strong $NDI^{\bullet-}$ signals by directly populating the NDI's LUMO in the ground state, irradiation of these samples does not enhance the $NDI^{\bullet-}$ signal intensity, indicating that anion-to-^{1}*NDI PET is turned OFF. On the other hand, when the thermal ET interactions are extremely weak or absent, $\pi\rightarrow\pi^*$ transition in NDIs opens the door for an energetically favored PET ($\Delta G^\circ_{PET} < 0$) from the anion's HOMO to the ^{1}*NDI's SOMO−1 level (Figure 1a). In control experiments, irradiation of NDIs in the absence of anions did not produce any $NDI^{\bullet-}$ radical anion (Figure S8), ruling out the possibilities of intramolecular or solvent-mediated PET.

Anion/NDI Charge-Transfer Interactions. While very weak Lewis basic I^- can reduce extremely strong π-acidic DCNDI to $DCNDI^{\bullet-}$, it does not produce any $NDI^{\bullet-}$ from weakly π-acidic *N,N′*-disubstituted NDIs via ET or PET. However, large excess of I^- (ca. 100 equiv) produces a characteristic CT band (λ_{CT} = 505 nm) with a concentrated solution of NDI **1** (the most π-acidic core-unsubstituted NDI in the series apart from DCNDI) in both ODCB and MeCN, but does not generate any $\mathbf{1}^{\bullet-}$ radical anion (Figure 6d). These observations further corroborate that, in aprotic solvents, I^- is indeed a weaker electron donor than strongly Lewis basic OH^- and F^- that form $NDI^{\bullet-}$ and NDI^{2-}. Thus, by adjusting the NDI's π-acidity and anion's Lewis basicity, the entire spectrum of ET, PET, and CT phenomena can be accessed (Figure 1).

2.5. NMR Titrations of NDIs with Anions. NMR experiments were conducted to determine the effects of anion/NDI interactions on their structural and electronic properties. ^{1}H NMR experiments can distinguish between the formation of either paramagnetic $NDI^{\bullet-}$ radical anions (NDI signals should disappear), covalent Meisenheimer complex (signals of originally symmetric NDIs should split because of the ensuing loss of symmetry), or CH···anion H-bonds (NDI signals should shift downfield). ^{19}F NMR experiments were introduced to gain insights into the nature of F^-/NDI interactions. If F^- reduces NDI to $NDI^{\bullet-}$ and NDI^{2-}, it should be oxidized into a paramagnetic $F^\bullet$ and the F^- signal should disappear. However, if a C–F σ-bond is formed in a diamagnetic $[F-NDI]^-$ Meisenheimer complex, it should display new F-signals. In the case of CH···F^- H-bonds, F^- signal should shift downfield. We looked for all this evidence to determine which mechanism actually takes place and to eliminate the others.

^{1}H NMR Titrations of N,N′-Disubstituted NDIs with Anions. The ^{1}H NMR spectrum of DPNDI (DMSO-d_6) shows a singlet at δ = 8.75 ppm corresponding to four identical NDI core protons (H_a) and two doublets at 7.58 and 8.81 ppm corresponding to H_b and H_c of two pyridine rings, respectively (Figure 7).[11a] During the titration with F^-, all DPNDI signals

dx.doi.org/10.1021/ja303173n | J. Am. Chem. Soc. 2012, 134, 13679–13691

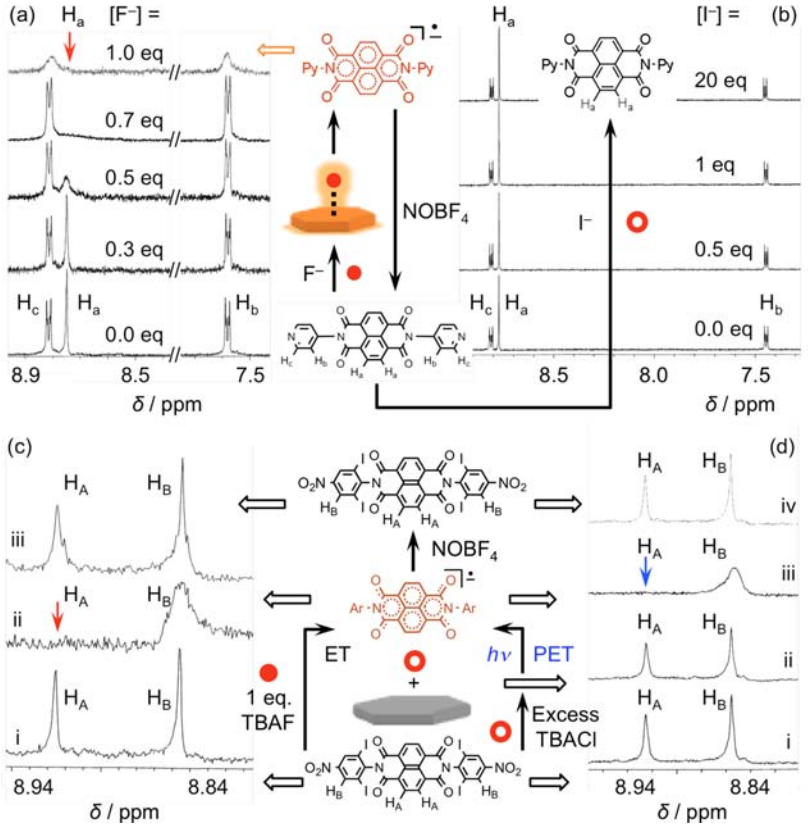

Figure 7. ^{1}H NMR titrations of DPNDI (DMSO-d_6, 298 K) with (a) F^- shows DPNDI$^{\bullet-}$ formation via thermal ET, as the H_a signal disappears and (b) excess I^- shows no DPNDI$^{\bullet-}$ formation. ^{1}H NMR spectra of NDI **1** (CD_3CN, 298 K) with (c) 1 equiv of F^- (trace ii) shows **1**$^{\bullet-}$ formation via thermal ET, as indicated by the disappearance of the H_A signal, and (d) excess Cl^- shows no **1**$^{\bullet-}$ formation through thermal ET in the dark (trace ii), but **1**$^{\bullet-}$ formation via PET (trace iii) upon irradiation with a W-lamp. In both cases, $NOBF_4$ oxidation of **1**$^{\bullet-}$ regenerated neutral NDI **1** [trace (iii) in (c) and trace (iv) in (d)].

became broad but none shifted at all, ruling out the possibility of a CH···F^- H-bond formation. At 1 equiv of F^-, H_a signal disappeared completely (Figure 7a), indicating the formation of a paramagnetic DPNDI$^{\bullet-}$ radical anion. EPR spectrum of this species confirmed the formation of DPNDI$^{\bullet-}$ radical anion (*vide infra*). The fact that the H_a signal does not split during the titration as a result of F^-/DPNDI interactions rules out the possibility of a covalent C−F bond formation. Had a diamagnetic, covalent [F−DPNDI]$^-$ Meisenheimer complex formed, the symmetry of DPNDI would have been destroyed, which should have caused splitting of the H_a signal. Oxidation of DPNDI$^{\bullet-}$ with $NOBF_4$ completely regenerated the original DPNDI spectrum, as the H_a signal returned to full glory (Figure 7a). Titrations of DPNDI with AcO^-, $H_2PO_4^-$, Cl^-, Br^-, and I^- ions did not cause any NMR spectroscopic change, even at high concentrations of anions (Figures 7b), confirming that these anions do not participate in ET with DPNDI.

Anion-induced thermal ET and PET to NDIs can also be distinguished by ^{1}H NMR experiments.[11b] ^{1}H NMR titrations of NDI **1** in CD_3CN demonstrate that while F^-, AcO^-, and $H_2PO_4^-$ generate paramagnetic **1**$^{\bullet-}$ through thermal ET, leading to the disappearance of its core H_A signal even in the dark (Figure 7c and S9), weaker Lewis basic Cl^- cannot do so in the absence of light (Figure 7d). Irradiation of NDI **1** in the presence of Cl^- quickly generates paramagnetic **1**$^{\bullet-}$ as its H_A signal disappears. Poor Lewis bases Br^- and I^- do not produce any NDI$^{\bullet-}$ radical anion via thermal ET or PET (Figure S9). The fact that, in the presence of electron-donating anions, NDI's H_A signal does not split or shift from its original position before disappearing rules out a nonsymmetric covalent anion−NDI intermediate formation or a CH···anion interaction involving H_A protons. Anion-generated NDI$^{\bullet-}$ radical anions are stable in dark, inert conditions, and they can be oxidized back to neutral NDI with $NOBF_4$, which brings the characteristic NDI signals back to full glory (Figures 7). Oxidative regeneration of NDIs confirms NDI$^{\bullet-}$ formation via ET in the first place and rules out a covalent Meisenheimer complex formation.

^{1}H NMR Titrations of DCNDI with Anions. To verify whether both F^- and I^- ions trigger ET to strongly π-acidic DCNDI generating DCNDI$^{\bullet-}$ in the same way or their interactions occur via different mechanisms, as predicted earlier,[8d] we conducted ^{1}H NMR titrations in CD_3CN. If I^- generated a paramagnetic DCNDI$^{\bullet-}$ radical anion via an ET, the NMR signals of DCNDI should disappear. On the other hand, if F^- formed a diamagnetic [F−DCNDI]$^-$ Meisenheimer complex via nucleophilic attack, the NMR signal of DCNDI core protons should split, since the symmetry of DCNDI would be lost as a result of a covalent C−F bond formation.

In CD_3CN, the aromatic region of symmetrical DCNDI displays a singlet at 9.07 ppm that corresponds to two core NDI protons (H_a), as well as a triplet centered on 7.38 ppm (H_c) and a doublet (H_b) at 7.30 ppm that correspond to the 2,6-dimethylphenyl substituents on imide N-centers. The H_a signal of DCNDI became broad and ultimately disappeared in the presence of 1 equiv of F^- or I^- anion without displaying any

dx.doi.org/10.1021/ja303173n | J. Am. Chem. Soc. 2012, 134, 13679−13691

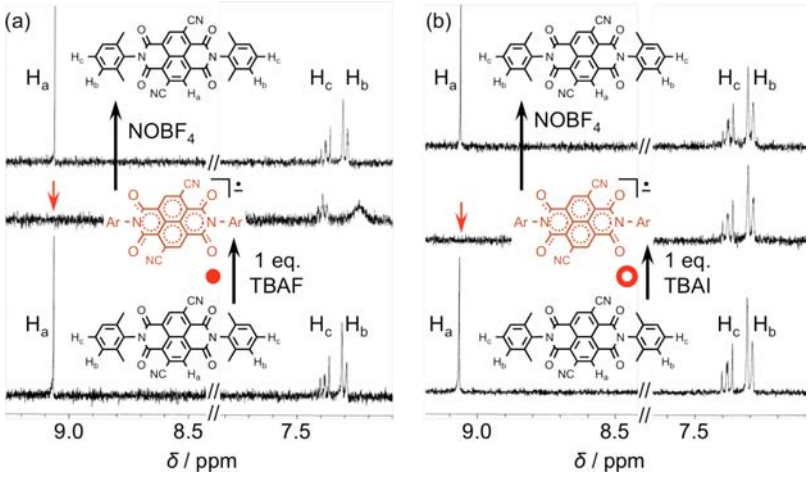

Figure 8. ^{1}H NMR spectra of DCNDI (CD_3CN, 298 K) before and after addition of (a) 1 equiv of F^- and (b) 1 equiv of I^-. Both generated paramagnetic $DCNDI^{\bullet-}$ radical anion as the H_a signal disappeared. $NOBF_4$ oxidized $DCNDI^{\bullet-}$ back to neutral DCNDI, regenerating the H_a signal.

splitting or shifting (Figure 8). The H_b and H_c signals also became broader but did not shift, split, or disappear. The anion-induced disappearance of H_a signal clearly indicates a paramagnetic $DCNDI^{\bullet-}$ radical anion formation with both F^- and I^-. The facts that both anions led to identical spectroscopic changes and the core DCNDI signal did not split with F^- ruled out a Meisenheimer complex formation. In both cases, all NMR signals returned to full glory after oxidation with $NOBF_4$ (Figure 8), demonstrating the reversibility of the entire process, which is consistent with an ET event. In the absence of core cyano substituents, less π-acidic NDIs do not generate $NDI^{\bullet-}$ with weakly basic I^- (Figure S10).

^{19}F NMR Studies. ^{19}F NMR spectrum of $TBAF{\cdot}3H_2O$ in DMSO-d_6 shows (Figure 9) a singlet peak at −102 ppm corresponding to the F^- ion and a doublet at −142.5 ppm that corresponds to HF_2^-.[11a,25] Titration of TBAF with DPNDI initially caused broadening and gradual upfield shift of the F^- signal (Figure 9), which disappeared completely in the presence of 1 equiv of DPNDI. While the upfield shift of F^- signal could be attributed to shielding by DPNDI π-system, its disappearance at 1:1 TBAF/DPNDI clearly indicates a $F^{\bullet}$ formation as a result of F^--induced ET to DPNDI that generates $DPNDI^{\bullet-}$ simultaneously. Although a C−F bond formation was considered as a possible alternative, no new F-signal corresponding to a new covalent C−F bond was found to

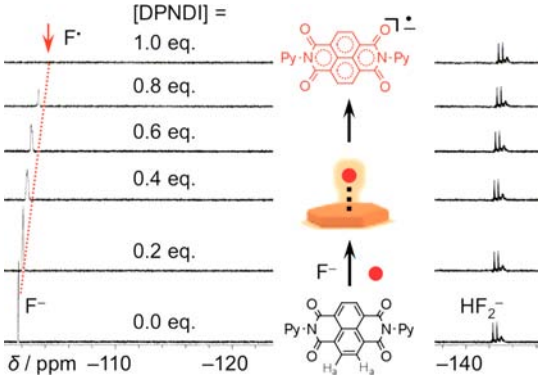

Figure 9. ^{19}F NMR titration (DMSO-d_6, 298 K) of $TBAF{\cdot}3H_2O$ with DPNDI, showing the disappearance of the F^- signal with 1 equiv of DPNDI, indicating a $F^{\bullet}$ formation.

support this scenario. The HF_2^- signal (−142.5 ppm) remained unaffected, and its intensity did not increase upon the addition of more and more DPNDI, ruling out a proton abstraction from the DPNDI, a process that should have generated more HF_2^- during the titration. Highly reactive $F^{\bullet}$ can rapidly react with silica, solvent, or counterions, making its capture into a well-defined product extremely difficult. Nevertheless, ^{19}F NMR spectroscopy shows $F^{\bullet}$ formation at the expense of F^-, and oxidative regeneration of neutral NDIs with $NOBF_4$ suggests that $F^{\bullet}$ or F^- does not covalently bind with NDIs at any stage.

Fate of Anions after ET. After ET, anion-generated $X^{\bullet}$ radicals act as sacrificial agents that could react with solvents, counterions, or, in case of $F^{\bullet}$, glassware (silica), forming strong Si−F bonds. The sacrificial nature of $X^{\bullet}$ radicals prevents $NDI^{\bullet-}$-to-$X^{\bullet}$ back-ET, allowing $NDI^{\bullet-}$ radical anions to persist in solutions for an extended time. Although radicals generated from inorganic anions (halides, OH^-) could not be trapped so far, the $F^{\bullet}$ formation at the expense of F^- has been observed through ^{19}F NMR spectroscopy. Since NDIs can be reduced to $NDI^{\bullet-}$ and NDI^{2-} by certain anions and $NOBF_4$ can oxidize them back to neutral NDIs, we examined whether $NOBF_4$ can directly oxidize OH^-, F^-, Cl^-, Br^-, and I^- anions (Figure S11). $NOBF_4$ treatment of these anions (as TBA^+ salts) emanated gases with characteristic colors (NO_2, brown; F_2, yellow; and Cl_2, greenish) and, in the case of Br^- and I^-, samples turned red and brown, respectively, (Br_2 and I_2).[26] Anions pretreated with $NOBF_4$ are already oxidized and can no longer reduce NDIs.

2.6. EPR Spectroscopy. EPR spectroscopy unequivocally confirms a paramagnetic $NDI^{\bullet-}$ radical anion formation via ET from strongly Lewis basic anions. While neutral DPNDI is diamagnetic and does not display any EPR signal, a 1:1 mixture of DPNDI and F^- in DMF displays characteristic EPR signals of delocalized $DPNDI^{\bullet-}$ radical anion (g = 2.0030)[11,22b] with hyperfine splitting patterns that match perfectly with the simulated EPR spectra of $DPNDI^{\bullet-}$ radical anion (Figure 10, orange trace). Excellent agreement between F^--generated and simulated $DPNDI^{\bullet-}$ EPR spectra indicates that F^- or $F^{\bullet}$ does not perturb the electronic and magnetic properties of $DPNDI^{\bullet-}$ radical anion. If a covalent $[F{-}DPNDI]^-$ Meisenheimer complex or a CH···F^- H-bonded complex were formed, it would have been a diamagnetic species and, therefore, should not have displayed any EPR signal.

dx.doi.org/10.1021/ja303173n | J. Am. Chem. Soc. 2012, 134, 13679−13691

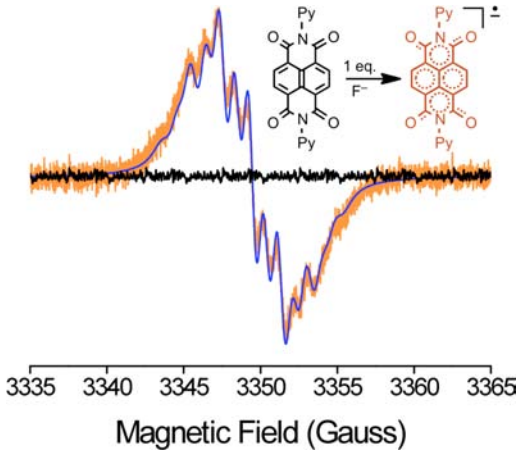

Figure 10. EPR spectrum (DMF, 298 K) of 1:1 DPNDI/F^- solution (orange trace) displays hyperfine splitting identical to a simulated $DPNDI^{\bullet-}$ spectrum (blue trace), confirming a paramagnetic $DPNDI^{\bullet-}$ formation (g = 2.0030) from diamagnetic DPNDI (black trace). Microwave frequency, 9.3902 GHz; power, 1 mW; and modulation amplitude, 1 G.

2.7. ITC Studies. ITC experiments were conducted to determine the stoichiometry, binding constants (K_a), and thermodynamic parameters (ΔH, $T\Delta S$, and ΔG) of anion/NDI interactions (Figure S12). ITC studies show exothermic 1:1 interactions between F^- and NDIs **1**−**5** with gradually decreasing K_a values (Table 2) as π-acidity of NDIs diminishes. Similarly, the anion affinity of NDI **1** diminishes with decreasing Lewis basicity of anions: $F^- > AcO^- > H_2PO_4^-$, as they show K_a's of 1230, 70, and 40 M^{-1}, respectively (ODCB, 298 K). Because of the presence of 2,6-iodo and fluoro groups at N-aryl rings, NDIs **1**, **2**, and **3** cannot form CH···anion H-bonds via the N-aryl substituents. Corroborating NMR and UV/vis data, stronger π-acidic NDIs **1**−**3** display greater F^- affinities than weaker π-acidic NDIs **4**−**7** that could potentially form CH···anion H-bonds involving 2,6-protons on their N-substituents. These results suggest that the affinity of anion/NDI interactions primarily depends on electron donor and acceptor strengths of anions and NDIs, respectively.

Table 2. Stoichiometry, K_a, and ΔG of Interactions between NDIs 1−7 and F^- in ODCB (298 K) Derived from ITC Analysis

NDI	NDI/F^- ratio	K_a (M^{-1})	ΔG (kcal/mol)
NDI **1**	1:1	1230	−4.24
NDI **2**	1:1	1080	−4.15
NDI **3**	1:1	923	−4.07
NDI **4**	1:1	708	−3.91
NDI **5**	1:1	528	−3.74

2.8. ESIMS Analysis. ESIMS provides physical evidence of anion/NDI binding, although it cannot differentiate between a noncovalent contact (CT, ET, or anion−π) and a covalent attachment, nor can it confirm whether a [X^-·NDI] precursor complex formation precedes a CT or ET event or a [$X^{\bullet}$·$NDI^{\bullet-}$] radical pair is formed as a result of the ET. ESIMS reveals (Figure S13) m/z signals of 1:1 complexes **1**·F^- (m/z 1030.9), **1**·AcO^- (1070.7), **1**·$H_2PO_4^-$ (1108.7), **2**·F^- (510.4), **2**·AcO^- (549.1), **2**·$H_2PO_4^-$ (587.0), **5**·F^- (437.1), and DPNDI·F^- (m/z 439.1), all of which led to the corresponding $NDI^{\bullet-}$ radical anion formation via ET. ESIMS also shows several 1:1 complexes of DPNDI (420.1) with weaker Lewis basic anions: Cl^- (455.1), Br^- (501.4), I^- (547.4), NO_2^- (466.1), NO_3^- (482.4), AcO^- (479.1), $PhCO_2^-$ (541.5), $H_2PO_4^-$ (517.4), HSO_4^- (517.4), ClO_4^- (519.4), and TfO^- (570.8), none of which triggered any CT or ET interactions, indicating that weak anion−π (anion−quadrupole) interactions are sufficient for the existence of these weak complexes. However, because of the lack of any measurable changes (*vide supra*), these weak interactions could not be quantified in solutions using UV/vis, NMR, and ITC experiments. ESIMS also shows $DPNDI^{2-}$ (m/z 210.4) formation in the presence of excess F^-, but due to electrostatic repulsion, it no longer binds any F^- ion.

2.9. XPS Analysis. XPS was introduced to further probe the nature (noncovalent vs covalent) of F^-/NDI interactions by measuring the binding energy of F_{1s} electrons in a 1:1 F^-/DPNDI mixture and comparing it with F-containing ionic and covalent compounds. F_{1s} electron binding energy is smaller for an ionic F^- salt than that of covalently bound fluorine. For example, F_{1s} binding energies in ionic CsF and NaF salts[27] and a fluorinated compound NDI **2** (containing covalent C−F bonds) are 682.2, 683.5, and 687.1 eV, respectively. F_{1s} binding energy measured for a 1:1 F^-/DPNDI mixture is 682.9 eV (Figure 11), which is in excellent agreement with that of ionic F^- compounds, indicating that no covalent C−F bond has been formed.

2.10. Computational and Structural Analysis. Electrostatic potential (ESP) maps of NDIs show that (Figure S14) the imide rings are the most electron-deficient areas. Consistent with the electron density map, B3LYP/6-31+G** energy minimization of anion·NDI complexes suggests that anions should preferentially interact with the electron-deficient imide rings (Figure S15). X-ray crystallographic analysis of a [Pd(II)−

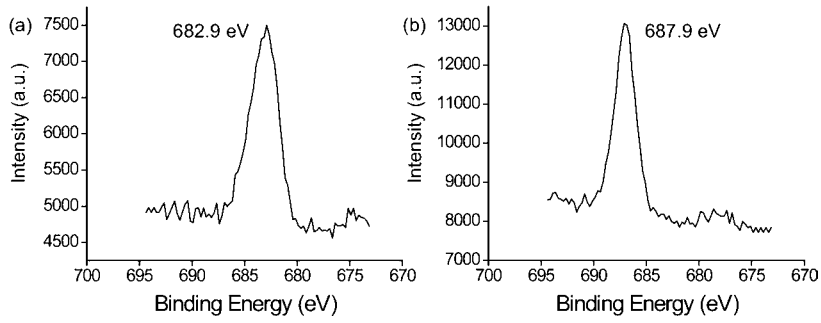

Figure 11. Comparison between F_{1s} XPS peak profiles of (a) 1:1 F^-/DPNDI mixture and (b) NDI **2** containing covalent C−F bonds indicates no C−F bond formation in (a).

DPNDI]$_n$ zigzag coordination polymer[28] reveals that oxygen lone-pair electrons of TfO^- counterions and THF molecules (solvent of crystallization) indeed interact with the electron-deficient imide rings of DPNDI ligands, albeit without participating in ET events. Calculated energy of F^-/DPNDI interaction in the gas phase is ca. 45 kcal/mol, which is comparable to a F−H···F^- H-bond (ca. 40 kcal/mol),[11a] but significantly weaker than a C−F covalent bond (ca. 115 kcal/mol). Furthermore, the shortest distance between a F^- ion and the carbonyl C-atom of DPNDI is 1.65 Å (Figure S15a), which is considerably longer than a typical C−F covalent bond (ca. 1.30 Å).

2.11. The Central Dogma. Consistent with the Lewis basicity trend of anions ($OH^- > F^- > CN^- > AcO^- > H_2PO_4^- > Cl^- > Br^- > I^-$),[23] all experimental results show that, in aprotic solvents, where smaller anions are not highly solvated, strongly Lewis basic anions (OH^-, F^-, CN^-, etc.) reduce DCNDI, DPNDI, and other NDIs to corresponding radical anion and dianion in two steps, whereas weaker Lewis basic anions (AcO^-, $H_2PO_4^-$, Cl^-, etc.) generate only $NDI^{\bullet-}$ radical anion from stronger π-acidic NDIs (e.g., DCNDI, NDIs **1** and **2**), and even less Lewis basic I^- can only reduce the most π-acidic DCNDI to $DCNDI^{\bullet-}$. However, these observations seemed counterintuitive to some critics because of a misconception that higher electronegativity of F, O, and N than I should render F^-, OH^-, and CN^- ions weaker electron donors than I^- in all solvents. It was insisted that better reducing ability of I^- over other anions in H_2O should be preserved universally in all solvents. While large, less solvated I^- acts as a good electron donor in H_2O,[12a] our studies clearly demonstrate that it is misleading to extrapolate this trend in aprotic organic solvents, in which Lewis basicity of less solvated F^-, OH^-, and CN^- ions is significantly higher. In aprotic solvents (ODCB, MeCN, DMF, and DMSO), highly Lewis basic F^- acts as a strong electron donor that can reduce NDIs to $NDI^{\bullet-}$ and NDI^{2-}, whereas in protic solvents, it becomes highly solvated and stabilized via H-bonding and loses its ability to reduce NDIs via ET. It is needless to say that electronegativity is an elemental property, which should not be misconstrued for the anion's electron-donating ability. Instead, it is Lewis basicity that reflects anion's electron-donating ability in aprotic solvents, in which stabilization of anions through solvation is minimum. Since all experimental evidence confirms the reduction of NDIs with strongly Lewis basic anions and rules out Meisenheimer complex formation and deprotonation of NDIs, the above-mentioned misconception led critics to offer alternative hypotheses for NDI reductions that would avoid ET from Lewis basic anions. To draw a clear picture and dispel any confusion, herein, we discuss these views and debunk them all with evidence and logic.

First, it was proposed that TBAX (X^- = OH^-, F^-, CN^-, AcO^-, Cl^-, etc. but ≠ I^-) could undergo β-elimination to form Bu_3N ($Bu_4N^+X^- \rightarrow Bu_3N + HX + CH_2{=}CHCH_2CH_3\uparrow$),[25] which would then reduce NDIs to corresponding $NDI^{\bullet-}$ and NDI^{2-} species. In control experiments, direct addition of Bu_3N and Et_3N to DPNDI did not produce any $DPNDI^{\bullet-}$ or $DPNDI^{2-}$ species, dismissing this hypothesis. An alternative hypothesis was that Lewis basic anions (X^- = F^-, OH^-, AcO^-) in TBAX salts could abstract an α-H, forming a $CH_3CH_2CH_2CH^-{-}{}^+NBu_3$ zwitterion (ylide) or other by-products, which could then act as a common reducing agent for NDIs. Even if this zwitterion is formed, which is unlikely and unknown, it is implausible that such a stable zwitterion would act as a better electron donor than strongly Lewis basic anions. If this zwitterion, its byproduct, or a carbanion generated via deprotonation of solvent (although unlikely) served as the common electron source instead of the original anions (X^-), then irrespective of anions, all TBAX salts should have produced the same species, i.e., either $NDI^{\bullet-}$ radical anion or NDI^{2-} dianion from all NDIs. Undermining this proposition, in aprotic solvents, TBA^+ and TEA^+ salts of stronger Lewis basic anions, e.g., F^- and OH^-, generate $NDI^{\bullet-}$ and NDI^{2-} in two steps, while weaker basic anions, e.g., AcO^-, $H_2PO_4^-$, and Cl^-, generate only $NDI^{\bullet-}$ radical anion from stronger π-acidic NDIs, and I^- can only produce $DCNDI^{\bullet-}$ radical anion from the most π-acidic DCNDI. Finally, it was suggested that F^- could deprotonate H_2O of $TBAF{\cdot}3H_2O$ to generate OH^-, which would then be responsible for the reduction of NDIs. According to the principles of acid−base chemistry, deprotonation of H_2O with F^- ($F^- + H_2O \leftrightarrows OH^- + HF$) is unlikely, since the equilibrium is favored toward the weaker conjugate acid, H_2O (pK_a in DMSO = 32), over the stronger conjugate acid HF (pK_a in DMSO = 15).[23] Some OH^- could exist in the equilibrium, and TBAOH itself is known to produce $NDI^{\bullet-}$ and NDI^{2-} species. However, the disappearance of F^- NMR signal in the presence of NDIs indicates $F^\bullet$ formation due to ET, and ITC and ESIMS data show a 1:1 $F^-{\cdot}$NDI complex formation, providing a clear indication that it is the F^- ion of TBAF, not OH^-, that reduces NDIs. Furthermore, $NOBF_4$-mediated oxidation of OH^-, F^-, Cl^-, Br^-, and I^- ions in solid phase and in MeCN demonstrates their electron-donating properties.[26] Thus, all experimental results corroborate that the electronegativity of elements does not accurately reflect the electron-donating ability of the corresponding anions in aprotic solvents. Effective size, electron-density, solvation, and electronic reorganization energy of anions obviously play major roles in their electron-donating abilities.

3. CONCLUSIONS

Powerful evidence obtained from UV/vis, NMR, and EPR spectroscopies, ITC, ESIMS, and XPS experiments all converge to show that, depending on the Lewis basicity of anions and π-acidity of NDIs, the nature of anion/NDI interactions ranges from extremely weak non-chromogenic anion−π interactions to anion-induced chromogenic charge-transfer, photoinduced electron-transfer, and thermal electron-transfer interactions. In spite of our conscious attempts to look for any evidence that could indicate the formation of covalent anion−NDI Meisenheimer complex or CH···anion H-bonded complex, none was found to support these alternative possibilities. When anions and NDIs are strong electron donors and acceptors, respectively, positioning the HOMO of an anion above the LUMO of an NDI, a thermal anion-to-NDI ET pathway is turned ON. When the HOMO of a weakly Lewis basic anion falls below the LUMO of an NDI but still lies above its HOMO, the thermal ET is turned OFF, but light can activate PET from the anion's HOMO to the photogenerated ^{1}*NDI's SOMO−1. Both pathways generate the same $NDI^{\bullet-}$ radical anions, as evident from identical spectroscopic signals. Anion/NDI CT interactions take place when anions are poor Lewis bases and cannot trigger ET or PET. In aprotic solvents, where stabilization of anions via solvation is minimum, electron-donating abilities of anions are dictated by their Lewis basicity. Thus, these comprehensive analyses not only depict a clear picture of how anions interact with NDIs under different conditions but also add a new paradigm to anion-recognition

chemistry, namely, anion-induced ET interactions. This knowledge could be exploited in various practical applications, ranging from anion sensing[11a] and fingerprinting to radical polymerization, NDI-based battery technology, conducting polymers, as well as molecular electronics and magnetism. Anion-induced ET to NDIs, generating $NDI^{\bullet-}$, could have undesired consequences during the synthesis of NDI-based conjugated polymers[29] and in other reactions involving NDI compounds. On the other hand, carboxylate-induced ET to strongly π-acidic NDIs could be exploited for biomimetic synthesis of neurotransmitters from α-amino acids via radical decarboxylation and initiation of radical polymerization, both of which are currently under study in our laboratory.

■ ASSOCIATED CONTENT

Supporting Information

Experimental section, and additional experimental and computational results. This material is available free of charge via the Internet at http://pubs.acs.org

■ AUTHOR INFORMATION

Corresponding Author

saha@chem.fsu.edu

Notes

The authors declare no competing financial interest.

■ ACKNOWLEDGMENTS

This research was supported by an ACS-PRF DNI grant (PRF no. 51737-DNI4) and FSU startup fund. We acknowledge Drs. Igor Alabugin, Naresh Dalal, and Vasant Ramachandran (FSU) for their assistance with computational analysis and EPR studies.

■ REFERENCES

(1) (a) Quiñonero, D.; Garau, C.; Rotger, C.; Frontera, A.; Ballester, P.; Costa, A.; Deya, P. M. *Angew. Chem., Int. Ed.* **2002**, *41*, 3389−3392. (b) Mascal, M.; Armstrong, A.; Bartberger, M. D. *J. Am. Chem. Soc.* **2002**, *124*, 6274−6276. (c) Alkorta, I.; Rozas, I.; Elguero, J. *J. Am. Chem. Soc.* **2002**, *124*, 8593−8598. (d) Garau, C.; Frontera, A.; Quinonero, D.; Ballester, P.; Costa, A.; Deya, P. M. *ChemPhysChem* **2003**, *4*, 1344−1348. (e) Berryman, O. B.; Bryantsev, V. S.; Stay, D. P.; Johnson, D. W.; Hay, B. P. *J. Am. Chem. Soc.* **2007**, *129*, 48−58. (f) Albrecht, M.; Wessel, C.; de Groot, M.; Rissanen, K.; Lüchow, A. *J. Am. Chem. Soc.* **2008**, *130*, 4600−4601. (g) White, N. G.; Kitchen, J. A.; Brooker, S. *Eur. J. Inorg. Chem.* **2009**, 1172−1180.

(2) (a) Schneider, H.-J.; Werner, F.; Blatter, T. *J. Phys. Org. Chem.* **1993**, *6*, 590−594. (b) de Hoog, P.; Gamez, P.; Mutikainen, I.; Turpeinen, U.; Reedijk, J. *Angew. Chem., Int. Ed.* **2004**, *43*, 5815−5817. (c) Campos-Fernández, C. S.; Schottel, B. L.; Chifotides, H. T.; Bera, J. K.; Bacsa, J.; Koomen, J. M.; Russell, D. H.; Dunbar, K. R. *J. Am. Chem. Soc.* **2005**, *127*, 12909−12923. (d) Gorteau, V.; Bollot, G.; Mareda, J.; Perez-Velasco, A.; Matile, S. *J. Am. Chem. Soc.* **2006**, *128*, 14788−14789. (e) Berryman, O. B.; Hof, F.; Hynesc, M. J.; Johnson, D. W. *Chem. Commun.* **2006**, 506−508. (f) Mascal, M.; Yakovlev, I.; Nikitin, E. B.; Fettinger, J. C. *Angew. Chem., Int. Ed.* **2007**, *46*, 8782−8784. (g) Berryman, O. B.; Johnson, D. W. *Chem. Commun.* **2009**, 3143−3153.

(3) (a) Gamez, P.; Mooibroek, T. J.; Teat, S. J.; Reedjik, J. *Acc. Chem. Res.* **2007**, *40*, 435−444. (b) Schottel, B. L.; Chifotides, H. T.; Dunbar, K. R. *Chem. Soc. Rev.* **2008**, *37*, 68−83. (c) Frontera, A.; Gamez, P.; Mascal, M.; Mooibroek, T. J.; Reedjik, J. *Angew. Chem., Int. Ed.* **2011**, *50*, 9564−9583. (d) Ballester, P. *Acc. Chem. Res.* **2012**, DOI: 10.1021/ar300080f.

(4) (a) Beer, P. D.; Gale, P. A. *Angew. Chem., Int. Ed.* **2001**, *40*, 486−516. (b) Sessler, J. L.; Gale, P. A.; Cho, W.-S. *Anion Receptor Chemistry*; RSC Publishing: London, 2006. (c) *Anion Coordination Chemistry*; Bowman-James, K., Bianchi, A., Garcia-Espana, E., Eds.; Wiley-Blackwell: New York, 2011. (d) Wenzel, M.; Hiscock, J. R.; Gale, P. A. *Chem. Soc. Rev.* **2012**, *41*, 480−520.

(5) (a) Lehn, J.-M.; Sonveaux, E.; Willard, A. K. *J. Am. Chem. Soc.* **1978**, *100*, 4914−4916. (b) Best, M. D.; Tobey, S. L.; Anslyn, E. V. *Coord. Chem. Rev.* **2003**, *240*, 3−15. (c) Cho, E. J.; Moon, J. W.; Ko, S. W.; Lee, J. Y.; Kim, S. K.; Yoon, J.; Nam, K. C. *J. Am. Chem. Soc.* **2003**, *125*, 12376−12377. (d) Custelcean, R.; Delmau, L. H.; Moyar, B. A.; Sessler, J. L.; Cho, W.-S.; Gross, D.; Bates, G. W.; Brooks, S. L.; Light, M. E.; Gale, P. A. *Angew. Chem., Int. Ed.* **2005**, *44*, 2537−2542. (e) Curiel, D.; Cowley, A.; Beer, P. D. *Chem. Commun.* **2005**, 236−238. (f) Kang, S. O.; Begum, R. A.; Bowman-James, K. *Angew. Chem., Int. Ed.* **2006**, *45*, 7882−7894. (g) Bhosale, S. V.; Bhosale, S. V.; Kalyankar, M. B.; Langford, S. J. *Org. Lett.* **2009**, *11*, 5418−5421.

(6) Wade, C. R.; Broomsgrove, A. E. J.; Aldridge, S.; Gabbaï, F. P. *Chem. Rev.* **2010**, *110*, 3958−3984.

(7) (a) Ma, J. C.; Dougherty, D. A. *Chem. Rev.* **1997**, *97*, 1303−1324. (b) Garau, C.; Frontera, A.; Quiñonero, D.; Ballester, P.; Costa, A.; Deya, P. M. *J. Phys. Chem. A* **2004**, *108*, 9423−9427.

(8) (a) Rosokha, Y. S.; Lindeman, S. V.; Rosokha, S. V.; Kochi, J. K. *Angew. Chem., Int. Ed.* **2004**, *43*, 4650 −4652. (b) Wang, D.-X.; Zheng, Q.-Y.; Wang, Q.-Q.; Wang, M.-X. *Angew. Chem., Int. Ed.* **2008**, *47*, 7485−7488. (c) Chifotides, H. T.; Schottel, B. L.; Dunbar, K. R. *Angew. Chem., Int. Ed.* **2010**, *49*, 7202−7207. (d) Dawson, R. E.; Henning, A.; Weimann, D. P.; Emery, D.; Ravikumar, V.; Montenegro, J.; Takeuchi, T.; Gabutti, S.; Mayor, M.; Mareda, J.; Schalley, C. A.; Matile, S. *Nat. Chem.* **2010**, *2*, 533−538.

(9) (a) Mulliken, R. S. *J. Am. Chem. Soc.* **1952**, *74*, 811−824. (b) Mulliken, R. S.; Person, W. B. *Molecular Complexes*; Wiley: New York, 1969.

(10) (a) Lokey, R. S.; Iverson, B. L. *Nature* **1995**, *375*, 303−305. (b) Iijima, T.; Vignon, S. A.; Tseng, H.-R.; Jarrosson, T.; Sanders, J. K. M.; Marchioni, F.; Venturi, M.; Apostoli, E.; Balzani, V.; Stoddart, J. F. *Chem.—Eur. J.* **2004**, *10*, 6375−6392. (c) Mukhopadhyay, P.; Iwashita, Y.; Shirakawa, M.; Kawano, S.-I.; Fujita, N.; Shinkai, S. *Angew. Chem., Int. Ed.* **2006**, *45*, 1592−1595. (d) Schneider, H.-J. *Angew. Chem., Int. Ed.* **2009**, *48*, 3924−3977.

(11) (a) Guha, S.; Saha, S. *J. Am. Chem. Soc.* **2010**, *132*, 17674−17677. (b) Guha, S.; Goodson, F. S.; Roy, S.; Corson, L. J.; Gravenmier, C.; Saha, S. *J. Am. Chem. Soc.* **2011**, *133*, 15256−15259.

(12) (a) Melby, L. R.; Harder, R. J.; Hertler, W. R.; Mahler, W.; Benson, R. E.; Mochel, W. E. *J. Am. Chem. Soc.* **1962**, *84*, 3374−3387. (b) Sun, D.; Rosokha, S. V.; Kochi, J. K. *J. Phys. Chem. B* **2007**, *111*, 6655−6666.

(13) Njus, D.; Jalukar, V.; Zu, J.; Kelley, P. M. *Am. J. Clin. Nutr.* **1991**, *54*, 1179S−1183S.

(14) Rostovtsev, V. V.; Green, L. G.; Fokin, V. V.; Sharpless, K. B. *Angew. Chem., Int. Ed.* **2002**, *41*, 2596−2599.

(15) (a) Berryman, O. B.; Bryantsev, V. S.; Stay, D. P.; Johnson, D. W.; Hay, B. P. *J. Am. Chem. Soc.* **2007**, *129*, 48−58. (b) Schneider, H.; Vogelhuber, K. M.; Schinle, F.; Weber, J. M. *J. Am. Chem. Soc.* **2007**, *129*, 13022−13026. (c) Hay, B. P.; Bryantsev, V. S. *Chem. Commun.* **2008**, 2417−2428. (d) Albrecht, M.; Muller, M.; Mergel, O.; Rissanen, K.; Valkonen, A. *Chem.—Eur. J.* **2010**, *16*, 5062−5069.

(16) (a) Mooibroek, T. J.; Black, C. A.; Gamez, P.; Reedijk, J. *Cryst. Growth Design* **2008**, *8*, 1082−1093. (b) Hay, B. P.; Custelcean, R. *Cryst. Growth Design* **2009**, *9*, 2539−2545.

(17) Li, Y.; Flood, A. H. *Angew. Chem., Int. Ed.* **2008**, *47*, 2649−2652.

(18) (a) Strauss, M. J. *Chem. Rev.* **1970**, *70*, 667−712. (b) Olson, E. J.; Xiong, T. T.; Cramer, C. J.; Bühlmann, P. *J. Am. Chem. Soc.* **2011**, *133*, 12858−12865.

(19) (a) Kim, D. Y.; Singh, N. J.; Lee, J. W.; Kim, K. S. *J. Chem. Theo. Comp.* **2008**, *4*, 1162−1169. (b) Campo-Cacharrón, A.; Cabaleiro-Lago, E. M.; Rodríguez-Otero, J. *ChemPhysChem* **2012**, *13*, 570−577.

(20) (a) Bhosale, S. V.; Janiab, C. H.; Langford, S. J. *Chem. Soc. Rev.* **2008**, *37*, 331−342. (b) Lin, N.-T.; Jentzsch, A. V.; Guénée, L.; Neudörfl, J.-M.; Aziz, S.; Berkessel, A.; Orentas, E.; Sakai, N.; Matile, S. *Chem. Sci.* **2012**, *3*, 1121−1127.

(21) (a) Thalacker, C.; Röger, C.; Würthner, F. *J. Org. Chem.* **2006**, *71*, 8098−8105. (b) Röger, C.; Würthner, F. *J. Org. Chem.* **2007**, *72*, 8070−8075. (c) Sakai, N.; Mareda, J.; Vauthey, E.; Matile, S. *Chem. Commun.* **2010**, *46*, 4225−4237. (d) Misek, J.; Jentzsch, A. V.; Sakurai, S.-I.; Emery, D.; Mareda, J.; Matile, S. *Angew. Chem., Int. Ed.* **2010**, *49*, 7680−7683.

(22) (a) Gosztola, D.; Niemczyk, M. P.; Svec, W.; Lukas, A. S.; Wasielewski, M. R. *J. Phys. Chem. A* **2000**, *104*, 6545−6551. (b) Andric, G.; Boas, J. F.; Bond, A. M.; Fallon, G. D.; Ghiggino, K. P.; Hogan, C. F.; Hutchison, J. A.; Lee, M. A.-P.; Langford, S. J.; Pilbrow, J. R.; Troup, G. J.; Woodward, C. P. *Aust. J. Chem.* **2004**, *57*, 1011−1019.

(23) (a) Huheey, J. E.; Keiter, E. A.; Keiter, R. L. *Inorganic Chemistry Principles of Structure and Reactivity*, 4th ed.; Harper Collins: New York, 1993; pp 332−333. (b) Anslyn, E. V.; Dougherty, D. A. *Modern Physical Organic Chemistry*; University Science Book: Sausalito, CA, 2006.

(24) Cametti, M.; Rissanen, K. *Chem. Commun.* **2009**, 2809−2829.

(25) Sun, H.; DiMagno, S. G. *J. Am. Chem. Soc.* **2005**, *127*, 2050−2051. While anhydrous TBAF may decompose through Hofmann elimination, TBAF·3H_2O does not. If TBAF·3H_2O generated a flammable 1-butene gas and Bu_3N via β-elimination, it would not be available in plastic containers from industrial manufacturers.

(26) Connelly, N. G.; Geiger, W. E. *Chem. Rev.* **1996**, *96*, 877−910. $NOBF_4$ (E_{Red} = +1.25 V vs SCE in MeCN) oxidizes colorless TBAX salts (X^- = OH^-, F^-, Cl^-, Br^-, I^-) in MeCN. $NOBF_4$ generates yellow and green gases from TBAF and TBACl, respectively, and turns colorless TBABr and TBAI solutions orange and brown, respectively, indicating the formation of the corresponding halogen molecules (Figure S11). Reduction of NO^+ with these anions should generate NO, which can be oxidized by O_2 to brown NO_2 gas. Emission of brown NO_2 fume is clearly visible with OH^-, when no other colored species is formed. Due to relatively low solubility of NDIs (mM) and an immediate formation of intensely colorful $NDI^{\bullet-}$ and NDI^{2-}, formation of X_2 by NDI could not be observed by the naked eye.

(27) Morgan, W. E.; Van Wazer, J. R.; Stec, W. J. *J. Am. Chem. Soc.* **1973**, *95*, 751−755.

(28) Guha, S.; Goodson, F. S.; Clark, J. R.; Saha, S. *CrystEngComm* **2012**, *14*, 1213−1215.

(29) Alvey, P. M.; Iverson, B. L. *Org. Lett.* **2012**, *14*, 2706−2709.